

Over-the-Air Federated Learning from Heterogeneous Data

Tomer Sery, Nir Shlezinger, Kobi Cohen, and Yonina C. Eldar

Abstract—Federated learning (FL) is a framework for distributed learning of centralized models. In FL, a set of edge devices train a model using their local data, while repeatedly exchanging their trained updates with a central server. This procedure allows tuning a centralized model in a distributed fashion without having the users share their possibly private data. In this paper, we focus on over-the-air (OTA) FL, which has been suggested recently to reduce the communication overhead of FL due to the repeated transmissions of the model updates by a large number of users over the wireless channel. In OTA FL, all users simultaneously transmit their updates as analog signals over a multiple access channel, and the server receives a superposition of the analog transmitted signals. However, this approach results in the channel noise directly affecting the optimization procedure, which may degrade the accuracy of the trained model. We develop a Convergent OTA FL (COTAF) algorithm which enhances the common local stochastic gradient descent (SGD) FL algorithm, introducing precoding at the users and scaling at the server, which gradually mitigates the effect of the noise. We analyze the convergence of COTAF to the loss minimizing model and quantify the effect of a statistically heterogeneous setup, i.e. when the training data of each user obeys a different distribution. Our analysis reveals the ability of COTAF to achieve a convergence rate similar to that achievable over error-free channels. Our simulations demonstrate the improved convergence of COTAF over vanilla OTA local SGD for training using non-synthetic datasets. Furthermore, we numerically show that the precoding induced by COTAF notably improves the convergence rate and the accuracy of models trained via OTA FL.

I. INTRODUCTION

Recent years have witnessed unprecedented success of machine learning methods in a broad range of applications [2]. These systems utilize highly parameterized models, such as deep neural networks (DNNs), trained using massive data sets. In many applications, samples are available at remote users, e.g. smartphones, and the common strategy is to gather these samples at a computationally powerful server, where the model is trained [3]. Often, data sets contain private information, and thus the user may not be willing to share them with the server. Furthermore, sharing massive data sets can result in a substantial burden on the communication links between the users and the server. To allow centralized training without data sharing, federated learning (FL) was proposed in [4] as a method combining

distributed training with central aggregation, and is the focus of growing research attention [5]. FL exploits the increased computational capabilities of modern edge devices to train a model on the users' side, having the server periodically synchronize these local models into a global one.

Two of the main challenges associated with FL are the heterogeneous nature of the data and the communication overhead induced by its training procedure [5]. Statistical heterogeneity arises when the data generating distributions vary between different sets of users [6]. This is typically the case in FL, as the data available at each user device is likely to be personalized towards the specific user. When training several instances of a model on multiple edge devices using heterogeneous data, each instance can be adapted to operate under a different statistical relationship, which may limit the inference accuracy of the global model [6]–[8].

The communication load of FL stems from the need to repeatedly convey a massive amount of model parameters between the server and a large number of users over wireless channels [8]. This is particularly relevant in uplink communications, which are typically more limited as compared to their downlink counterparts [9]. A common strategy to tackle this challenge is to reduce the amount of data exchanges between the users and the server, either by reducing the number of participating users [10], [11], or by compressing the model parameters via quantization [12], [13] or sparsification [14], [15]. All these methods treat the wireless channel as a set of independent error-free bit-limited links between the users and the server. As wireless channels are shared and noisy [16], a common way to achieve such communications is to divide the channel resources among users, e.g., by using frequency division multiplexing (FDM), and have the users utilize channel codes to overcome the noise. This, however, results in each user being assigned a dedicated band whose width decreases with the number of users, which in turn increases the energy consumption required to meet a desirable communication rate and decreases the overall throughput and training speed.

An alternative FL approach is to allow the users to simultaneously utilize the complete temporal and spectral resources of the uplink channel in a non-orthogonal manner. In this method, referred to as over-the-air (OTA) FL [17]–[21], the users transmit their model updates via analog signalling, i.e., without converting to discrete coded symbols which should be decoded at the server side. Such FL schemes exploit the inherent aggregation carried out by the shared channel as a form of OTA computation [22]. This strategy builds upon the fact that when the participating users operate over the same wireless network, uplink transmissions are carried out over a multiple access channel (MAC). Model-dependent inference over MACs is relatively well-studied in the sensor network literature, where methods

A short version of this paper that introduces the algorithm for i.i.d. data and preliminary simulation results was accepted for presentation in the 2020 IEEE Global Communications Conference (GLOBECOM) [1]. This research was supported by the Benoziyo Endowment Fund for the Advancement of Science, the Estate of Olga Klein – Astrachan, the European Union's Horizon 2020 research and innovation program under grant No. 646804-ERC-COG-BNYQ, the Israel Science Foundation under grant No. 0100101, the Israel Science Foundation under grant No. 2640/20, and the U.S.-Israel Binational Science Foundation (BSF) under grant No. 2017723. T. Sery, N. Shlezinger, and K. Cohen are with the School of Electrical and Computer Engineering, Ben-Gurion University of the Negev, Beer-Sheva, Israel (e-mail: seryt@post.bgu.ac.il; {nirshl, yakovsec}@bgu.ac.il). Y. C. Eldar is with the Math and CS Faculty, Weizmann Institute of Science, Rehovot, Israel (e-mail: yonina.eldar@weizmann.ac.il).

for model-dependent inference over MACs and theoretical performance guarantees have been established under a wide class of problem settings [23]–[32]. These studies focused on model-based inference, and not on machine learning paradigms. In the context of FL, which is a distributed machine learning setup, with OTA computations, the works [17], [18] considered scenarios where the model updates are sparse with an identical sparsity pattern, which is not likely to hold when the data is heterogeneous. Additional related recent works on OTA FL, including [19], [21], [33], [34], considered the distributed application of full gradient descent optimization over noisy channels. While distributed learning based on full gradient descent admits a simplified and analytically tractable analysis, it is also less communication and computation efficient compared to local stochastic gradient descent (SGD), which is the dominant optimization scheme used in FL [4], [5]. Consequently, the OTA FL schemes proposed in these previous works and the corresponding analysis of their convergence may not reflect the common application of FL systems, i.e., distributed training with heterogeneous data via local SGD.

The main advantage of OTA FL is that it enables the users to transmit at increased throughput, being allowed to utilize the complete available bandwidth regardless of the number of participating users. However, a major drawback of such uncoded analog signalling is that the noise induced by the channel is not handled by channel coding and thus affects the training procedure. In particular, the accuracy of learning algorithms such as SGD is known to be sensitive to noisy observations, as in the presence of noise the model can only be shown to converge to some environment of the optimal solution [35]. Combining the sensitivity to noisy observations with the limited accuracy due to statistical heterogeneity of FL systems, implies that conventional FL algorithms, such as local SGD [36], exhibit degraded performance when combined with OTA computations, and are unable to converge to the optimum. This motivates the design and analysis of an FL scheme for wireless channels that exploit the high throughput of OTA computations, while preserving the convergence properties of conventional FL methods designed for noise-free channels.

Here, we propose the convergent OTA FL (COTAF) algorithm which introduces precoding and scaling laws. COTAF facilitates high throughput FL over wireless channels, while preserving the accuracy and convergence properties of the common local SGD method for distributed learning. Being an OTA FL scheme, COTAF overcomes the need to divide the channel resources among the users by allowing the users to simultaneously share the uplink channel, while aggregating the global model via OTA computations. To guarantee convergence to an accurate parameter model, we introduce time-varying precoding to the transmitted signals, which accounts for the fact that the expected difference in each set of SGD iterations is expected to gradually decrease over time. Building upon this insight, COTAF scales the model updates by their maximal expected norm, along with a corresponding aggregation mapping at the server side, which jointly results in an equivalent model where the effect of the noise induced by the channel is mitigated over time.

We theoretically analyze the convergence of machine learning models trained by COTAF to the minimal achievable loss function in the presence of heterogeneous data. Our theoretical analysis focuses on scenarios in which the objective function is strongly convex and smooth, and the stochastic gradients have bounded variance. Under such scenarios, which are commonly utilized in FL convergence studies over error-free channels [11], [36], [37], noise degrades the ability to converge to the global optimum.

We provide three convergence bounds: The first characterizes the distance between a weighted average of past models trained in a federated manner [36]; The second treats the convergence of the instantaneous model available at the end of the FL procedure [11]. The first two bounds consider FL over non-fading channels. We then extend COTAF for fading channels and characterize the corresponding convergence of the instantaneous model. Our analysis proves that when applying COTAF, the usage of analog transmissions over shared noisy channels does not affect the asymptotic convergence rate of local SGD compared to FL over error-free separate channels, while allowing the users to communicate at high throughput by avoiding the need to divide the channel resources. Our convergence bounds show that the distance to the desired model is smaller when the data is closer to being i.i.d., as in FL over error-free channels with heterogeneous data [11]. Unlike previous convergence proofs of OTA FL, our analysis of COTAF is not restricted to sparsified updates as in [20] or to full gradient descent optimization as in [21], and holds for the typical FL setting with SGD-based training and heterogeneous data.

We evaluate COTAF in two scenarios involving non-synthetic data sets: First, we train a linear estimator, for which the objective function is strongly convex, with the Million Song Dataset [38]. In such settings we demonstrate that COTAF achieves accuracy within a minor gap from that of noise-free local SGD, while notably outperforming OTA FL strategies without time-varying precoding designed to facilitate convergence. Then, we train a convolutional neural network (CNN) over the CIFAR-10 dataset, representing a deep FL setup with a non-convex objective, for which a minor level of noise is known to contribute to convergence as means of avoiding local mimimas [39]. We demonstrate that COTAF improves the accuracy of trained models when using both i.i.d and heterogeneous data. Here, COTAF benefits from the presence of the gradually mitigated noise to achieve improved performance not only over conventional OTA FL, but also over noise-free local SGD.

The rest of this paper is organized as follows: Section II briefly reviews the local SGD algorithm and presents the system model of OTA FL. Section III presents the COTAF scheme along with its theoretical convergence analysis. Numerical results are detailed in Section IV. Finally, Section V provides concluding remarks. Detailed proofs of our main results are given in the appendix.

Throughout the paper, we use boldface lower-case letters for vectors, e.g., \mathbf{x} . The ℓ_2 norm, stochastic expectation, and Gaussian distribution are denoted by $\|\cdot\|$, $\mathbb{E}[\cdot]$, and $\mathcal{N}(\cdot, \cdot)$ respectively. Finally, \mathbf{I}_n is the $n \times n$ identity matrix, and \mathbb{R} is the set of real numbers.

II. SYSTEM MODEL

In this section we detail the system model for which COTAF is derived in the following section. We first formulate the objective of FL in Subsection II-A. Then, Subsection II-B presents the communication channel model over which FL is carried out. We briefly discuss the local SGD method, which is the common FL algorithm, in Subsection II-C, and formulate the problem in Subsection II-D.

A. Federated Learning

We consider a central server which trains a model consisting of d parameters, represented by the vector $\theta \in \Theta \subset \mathbb{R}^d$, using data available at N users, indexed by the set $\mathcal{N} = \{1, 2, \dots, N\}$, as illustrated in Fig. 1. Each user of index $n \in \mathcal{N}$ has access to a data set of D_n entities, denoted by $\{s_i^n\}_{i=1}^{D_n}$, sampled in an i.i.d. fashion from a local distribution \mathcal{X}_n . The users can communicate with the central server over a wireless channel formulated in Subsection II-B, but are not allowed to share their data with the server.

To define the learning objective, we use $l(\cdot, \theta)$ to denote the loss function of a model parameterized by θ . The empirical loss of the n th user is defined by

$$f_n(\theta) \triangleq \frac{1}{D_n} \sum_{i=1}^{D_n} l(s_i^n; \theta). \quad (1)$$

The objective is the average global loss, given by

$$F(\theta) \triangleq \frac{1}{N} \sum_{n=1}^N f_n(\theta). \quad (2)$$

Therefore, FL aims at recovering

$$\theta^* \triangleq \arg \min_{\theta \in \Theta} F(\theta). \quad (3)$$

When the data is homogeneous, i.e., the local distributions $\{\mathcal{X}_n\}$ are identical, the local loss functions converge to the same expected loss measure on the horizon of a large number of samples $D_n \rightarrow \infty$. However, the statistical heterogeneity of FL, i.e., the fact that each user observes data from a different distribution, implies that the parameter vectors which minimize the local loss vary between different users. This property generally affects the behavior of the learning method used in FL, such as the common local SGD algorithm, detailed in Subsection II-C.

B. Communication Channel Model

FL is often carried out over wireless channels. We consider FL setups in which the N users communicate with the server using the same wireless network, either directly or via some wireless access point. As uplink communications, i.e., from the users to the server, is typically notably more constrained as compared to its downlink counterpart in terms of throughput [9], we focus on uplink transmissions over MAC. The downlink channel is modeled as supporting reliable communications at arbitrary rates, as commonly assumed in FL studies [12]–[15], [17]–[19], [40].

We next formulate the uplink channel model. Wireless channels are inherently a shared and noisy media, hence

the channel output received by the server at time instance t when each user transmits a $d \times 1$ vector \mathbf{x}_t^n is given by

$$\mathbf{y}_t = \sum_{n=1}^N \mathbf{x}_t^n + \tilde{\mathbf{w}}_t, \quad (4)$$

where $\tilde{\mathbf{w}}_t \sim \mathcal{N}(0, \sigma_w^2 \mathbf{I}_d)$ is $d \times 1$ vector of additive noise. The channel input is subject to an average power constraint

$$\mathbb{E}[\|\mathbf{x}_t^n\|^2] \leq P, \quad (5)$$

where $P > 0$ represents the available transmission power. The channel in (4) represents an additive noise MAC, whose main resources are its spectral band, denoted B , and its temporal blocklength τ , namely, \mathbf{y}_t is obtained by observing the channel output over the bandwidth B for a duration of τ time instances.

The common approach in wireless communication protocols and in FL research is to overcome the mutual interference induced in the shared wireless channels by dividing the bandwidth into multiple orthogonal channels. This can be achieved by, e.g., FDM, where the bandwidth is divided into N distinct bands, or via time division multiplexing (TDM), in which the temporal block is divided into N slots which are allocated among the users. In such cases, the server has access to a distinct channel output for each user, of the form

$$\mathbf{y}_t^n = \mathbf{x}_t^n + \tilde{\mathbf{w}}_t^n, \quad n \in \mathcal{N}. \quad (6)$$

The orthogonalization of the channels in (6) facilitates recovery of each \mathbf{x}_t^n individually. However, the fact that each user has access only to $1/N$ of the channel resources implies that its throughput, i.e., the volume of data that can be conveyed reliably, is reduced accordingly [16, Ch. 4]. In order to facilitate high throughput FL, we do not restrict the users to orthogonal communication channels, and thus the server has access to the shared channel output (4) rather than the set of individual channel outputs in (6).

We derive our OTA FL scheme and analyze its performance assuming that the users communicate with the server of the noisy MAC (4). However, in practice wireless channels often induce fading in addition to noise. Each user of index n experiences at time t a block fading channel $\tilde{h}_t^n = h_t^n e^{j\phi_t^n}$, where $h_t^n > 0$ and $\phi_t^n \in [-\pi, \pi]$ are its magnitude and phase, respectively. In such cases, the channel input-output relationship is given by

$$\mathbf{y}_t = \sum_{n=1}^N \tilde{h}_t^n \mathbf{x}_t^n + \tilde{\mathbf{w}}_t. \quad (7)$$

Therefore, while our derivation and analysis focuses on additive noise MACs as in (4), we also show how the proposed COTAF algorithm can be extended to fading MACs of the form (7). In our extension, we assume that the participating entities have channel state information (CSI), i.e., knowledge of the fading coefficients. Such knowledge can be obtained by letting the users sense their channels, or alternatively by having the access point/server periodically estimate these coefficients and convey them to the users.

C. Local SGD

Local SGD, also referred to as *federated averaging* [4], is a distributed learning algorithm aimed at recovering (3),

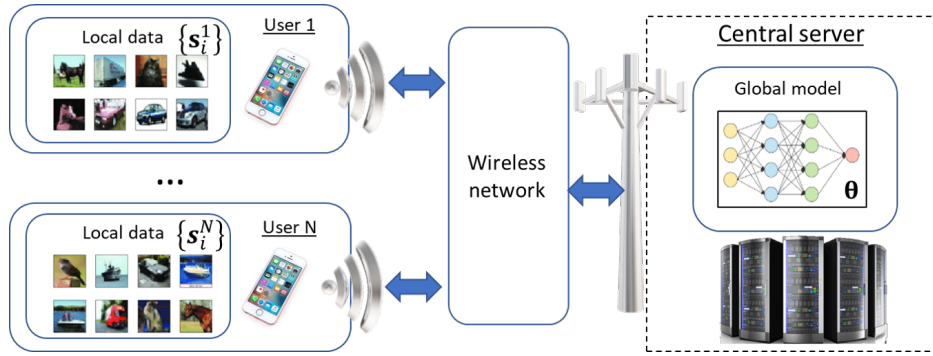


Fig. 1. An illustration of the distributed optimization setup. In this example, the data consists of images, where those of user 1 are biased towards car images, while those of user N contain a large portion of ship images, resulting in a heterogeneous setup.

without having the users share their local data. This is achieved by carrying out multiple training rounds, each consisting of the following three phases:

- 1) The server shares its current model at time instance t , denoted by θ_t , with the users.
- 2) Each user sets its local model θ_t^n to θ_t , and trains it using its local data set over H SGD steps, namely,

$$\theta_{t+1}^n = \theta_t^n - \eta_t \nabla f_{i_t^n}(\theta_t^n), \quad (8)$$

where $f_{i_t^n}(\theta) \triangleq l(s_{i_t^n}^n; \theta)$ is the loss evaluated at a single data sample, drawn uniformly from $\{s_i^n\}_{i=1}^{D_n}$, and η_t is the SGD step size. The update rule (8) is repeated H steps to yield θ_{t+H}^n .

- 3) Each user conveys its trained local model θ_{t+H}^n (or alternatively, the updates in its trained model $\theta_{t+H}^n - \theta_t^n$) to the central server, which averages them into a global model via¹ $\theta_{t+H} = \frac{1}{N} \sum_{n=1}^N \theta_{t+H}^n$, and sends the new model to the users for another round.

The uplink transmission in this algorithm is typically executed over an error-free channel with limited throughput, where channel noise and fading are assumed to be eliminated [11], [36], [37]. The local SGD algorithm is known to result in a model θ_t whose objective function $F(\theta_t)$ converges to $F^* \triangleq F(\theta^*)$ as the number of rounds grows for various families of loss measures under homogeneous data [36]. When the data is heterogeneous, convergence is affected by an additional term encapsulating the *degree of heterogeneity*, defined as $\Gamma \triangleq F^* - \frac{1}{N} \sum_{n=1}^N f_n^*$, where $f_n^* \triangleq \min_{\theta} f_n(\theta)$ [11]. In particular, for convex objectives, convergence of the global model to (3) can be still guaranteed, though at slower rates compared to homogeneous setups [11]. To the best of our knowledge, the convergence of local SGD with heterogeneous data carried out over noisy fading wireless channels has not been studied to date.

D. Problem Formulation

Local SGD, as detailed in the previous subsection, is the leading learning algorithm in FL. Each round of local SGD consists of two communication phases: downlink transmission of the global model θ_t from the server to the users, and uplink transmissions of the updated local models $\{\theta_{t+H}^n\}$ from each user to the server. An illustration of

¹While we focus here on conventional averaging of the local models, our framework can be naturally extended to weighted averages.

a single round of local SGD carried out over a wireless MAC of the form (4) is depicted in Fig. 2. This involves the repetitive communication of a large amount of parameters over wireless channels. This increased communication overhead is considered one of the main challenges of FL [5], [8]. The conventional strategy in the FL literature is to treat the uplink channel as an error-free bit-constrained pipeline, and thus the focus is on deriving methods for compressing and sparsifying the conveyed model updates, such that convergence of θ_t to θ^* is preserved [12], [13], [15]. However, the model of error-free channels, which are only constrained in terms of throughput, requires the bandwidth of the wireless channel to be divided between the users and have each user utilize coding schemes with a rate small enough to guarantee accurate recovery. This severely limits the volume of data which can be conveyed as compared to utilizing the full bandwidth.

The task of the server on every communication round in FL is not to recover each model update individually, but to aggregate them into a global model θ_t . This motivates having each of the users exploit the complete spectral and temporal resources by avoiding conventional orthogonality-based strategies and utilizing the wireless MAC (4) on uplink transmissions. The inherent aggregation carried out by the MAC can in fact facilitate FL at high communication rate via OTA computations [22], as was also proposed in the context of distributed learning in [17]–[19]. However, the fact that the channel outputs are corrupted by additive noise is known to degrade the ability of SGD-based algorithms to converge to the desired θ^* for convex objectives [35], adding to the inherent degradation due to statistical heterogeneity. For non-convex objectives, noise can contribute to the overall convergence as it reduces the probability of getting trapped in local minima [39], [41]. However, for the learning algorithm to benefit from such additive noise, the level of noise should be limited. It is preferable to have a gradual decay of the noise over time to allow convergence when in the proximity of the desired optimum point, which is not the case when communicating over noisy MACs.

Our goal is to design a communication strategy for FL over wireless channels of the form (4). This involves determining a mapping, referred to as precoding, from θ_t^n into x_t^n at each user, as well as a transformation of y_t into θ_t on the server side. The protocol is required to: 1) Mitigate the limited convergence of noisy SGD for convex

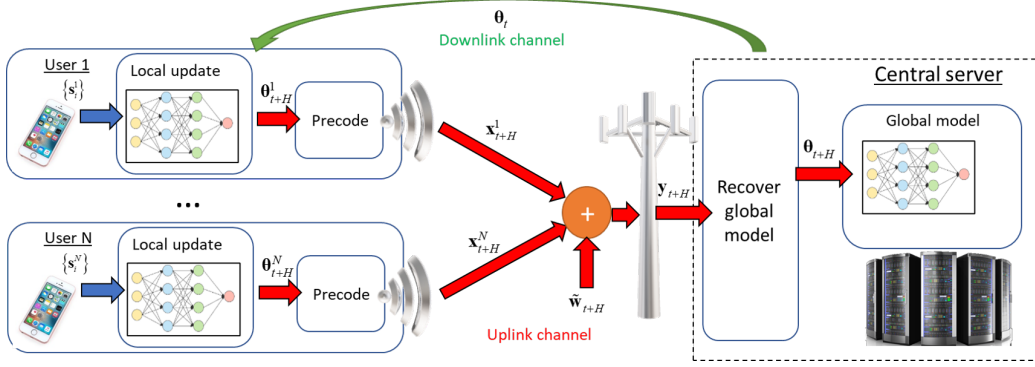


Fig. 2. An illustration of FL over wireless MAC.

objectives by properly precoding the model updates into the channel inputs $\{\mathbf{x}_t^n\}$; 2) benefit from the presence of noise when trained using non-convex objectives; and 3) allow achieving FL performance which approaches that of FL over noise-free orthogonal channels for convex objectives, while utilizing the complete spectral and temporal resources of the wireless channel. This is achieved by introducing time-varying precoding mapping $\theta_t^n \mapsto \mathbf{x}_t^n$ at the users' side which accounts for the fact that the parameters are conveyed in order to be aggregated into a global model. Scaling laws are introduced at the server side for accurate transformation of the received signal to a global model. These rules gradually mitigate the effect of the noise on the resulting global model, as detailed in the following section.

III. THE CONVERGENT OVER-THE-AIR FEDERATED LEARNING (COTAF) ALGORITHM

In this section, we propose the COTAF algorithm. We first describe the COTAF transmission and aggregation protocol in Subsection III-A. Then, we analyze its convergence in Subsection III-B, proving its ability to converge to the loss-minimizing network weights under strongly convex objectives. In Subsection III-C we extend COTAF to fading channels, and discuss its pros and cons in Subsection III-D.

A. Precoding and Reception Algorithm

In COTAF, all users transmit their corresponding signals $\{\mathbf{x}_t^n\}$ over a shared channel to the server, thus the transmitted signals are aggregated over the wireless MAC and are received as a sum, together with additive noise, at the server. As in [17], [19], [25], we utilize analog signalling, namely, each vector \mathbf{x}_t^n consists of continuous-amplitude quantities, rather than a set of discrete symbols or bits, as common in digital communications. On each communication round, the server recovers the global model directly from the channel output \mathbf{y}_t as detailed in the sequel, and feeds back the updated model to the users as in conventional local SGD.

COTAF implements the local SGD algorithm while communicating over an uplink wireless MAC as illustrated in Fig. 2. Let \mathcal{H} be the set of time instances in which transmissions occur, i.e., the integer multiples of H . In order to convey the local trained model after H local SGD steps, i.e., at time instance $t \in \mathcal{H}$, the n th user precodes its model update $\theta_t^n - \theta_{t-H}^n$ into the MAC channel input \mathbf{x}_t^n via

$$\mathbf{x}_t^n = \sqrt{\alpha_t} (\theta_t^n - \theta_{t-H}^n), \quad (9)$$

where α_t is a precoding factor set to gradually amplify the model updates as t progresses, while satisfying the power constraint (5). The precoder α_t is given by

$$\alpha_t \triangleq \frac{P}{\max_n \mathbb{E} [\|\theta_t^n - \theta_{t-H}^n\|^2]}. \quad (10)$$

The precoding parameter α_t depends on the distribution of the updated model, which depends on the distribution of the data. It can thus be computed by performing offline simulations with smaller data sets and distributing the numerically computed coefficients among the users, as we do in our numerical study in Section IV. Alternatively, when the loss function has bounded gradients, this term can be replaced with a coefficient that is determined by the bound on the norm of the gradients, as we discuss in Subsection III-D.

The channel output (4) is thus given by

$$\mathbf{y}_t = \sum_{n=1}^N \sqrt{\alpha_t} (\theta_t^n - \theta_{t-H}^n) + \tilde{\mathbf{w}}_t. \quad (11)$$

In order to recover the aggregated global model θ_t from \mathbf{y}_t , the server sets

$$\theta_t = \frac{\mathbf{y}_t}{N\sqrt{\alpha_t}} + \theta_{t-H}, \quad (12)$$

for $t \in \mathcal{H}$, where θ_0 is the initial parameter estimate. The global update rule (12) can be equivalently written as

$$\theta_t = \frac{1}{N} \sum_{n=1}^N \theta_t^n + \mathbf{w}_t, \quad (13)$$

where $\mathbf{w}_t \triangleq \frac{\tilde{\mathbf{w}}_t}{N\sqrt{\alpha_t}}$ is the equivalent additive noise term distributed via $\mathbf{w}_t \sim \mathcal{N}(0, \frac{\sigma_w^2}{N^2\alpha_t} \mathbf{I}_d)$. The resulting OTA FL algorithm with R communication rounds is summarized below in Algorithm 1. Here, the local model available at the n th user at time t can be written as:

$$\theta_{t+1}^n = \begin{cases} \theta_t^n - \eta_t \nabla f_{i_t^n}(\theta_t^n), & t+1 \notin \mathcal{H}, \\ \frac{1}{N} \sum_{n=1}^N (\theta_t^n - \eta_t \nabla f_{i_t^n}(\theta_t^n)) + \mathbf{w}_t, & t+1 \in \mathcal{H}. \end{cases} \quad (14)$$

B. Performance Analysis

In this section, we theoretically characterize the convergence of COTAF to the optimal model parameters θ^* , i.e., the vector θ which minimizes the global loss function. Our analysis is carried out under the following assumptions:

Algorithm 1: COTAF algorithm

Init: Fix an initial $\theta_0^n = \theta_0$ for each user $n \in \mathcal{N}$.

1 **for** $t = 1, 2, \dots, RH$ **do**

2 Each user $n \in \mathcal{N}$ locally trains θ_t^n via (8);

3 **if** $t \in \mathcal{H}$ **then**

4 Each user $n \in \mathcal{N}$ transmits x_t^n precoded via (9) over the MAC (4);

5 The server recovers θ_t from y_t via (12);

6 The server broadcasts θ_t to the users;

7 Each user $n \in \mathcal{N}$ sets $\theta_t^n = \theta_t$;

8 **end**

9 **end**

Output: Global model θ_{RH}

- AS1 The objective function $F(\cdot)$ is L -smooth, namely, for all $\mathbf{v}_1, \mathbf{v}_2$ it holds that $F(\mathbf{v}_1) - F(\mathbf{v}_2) \leq (\mathbf{v}_1 - \mathbf{v}_2)^T \nabla F(\mathbf{v}_2) + \frac{1}{2}L\|\mathbf{v}_1 - \mathbf{v}_2\|^2$.
- AS2 The objective function $F(\cdot)$ is μ -strongly convex, namely, for all $\mathbf{v}_1, \mathbf{v}_2$ it holds that $F(\mathbf{v}_1) - F(\mathbf{v}_2) \geq (\mathbf{v}_1 - \mathbf{v}_2)^T \nabla F(\mathbf{v}_2) + \frac{1}{2}\mu\|\mathbf{v}_1 - \mathbf{v}_2\|^2$.
- AS3 The stochastic gradients $\nabla f_{i_t^n}(\theta)$ satisfy $\mathbb{E}[\|\nabla f_{i_t^n}(\theta)\|^2] \leq G^2$ and $\mathbb{E}[\|\nabla f_{i_t^n}(\theta) - \nabla f_n(\theta)\|^2] \leq M_n^2$ for some fixed $G^2 > 0$ and $M_n^2 > 0$, for each $\theta \in \Theta$ and $n \in \mathcal{N}$.

Assumptions *AS1-AS3* are commonly used when studying the convergence of FL schemes, see, e.g., [11], [36]. In particular, *AS1-AS2* hold for a broad range of objective functions used in FL systems, including ℓ_2 -norm regularized linear regression and logistic regression [11], while *AS3* represents having bounded second-order statistical moments of the stochastic gradients [36]. Convergence proofs for such scenarios are of particular interest in the presence of noise, such as that introduced by the wireless channel in OTA FL, as noise is known to degrade the ability of local SGD to converge to θ^* . It is also emphasized that these assumptions are required to maintain an analytically tractable convergence analysis, and that COTAF can be applied for arbitrary learning tasks for which *AS1-AS3* do not necessarily hold, as numerically demonstrated in Section IV.

After $T = RH$ iterations of updating the global model via COTAF, the server can utilize its learned global model for inference. This can be achieved by setting the global model weights according to the instantaneous parameters vector available at this time instance, i.e., θ_T . An alternative approach is to utilize the fact that the server also has access to previous aggregated models, i.e., $\{\theta_r\}$ for each $r \in \mathcal{H}$ such that $r \leq T$. In this case, the server can infer using a model whose parameters are obtained as a weighted average of its previous learned model parameters, denoted by $\hat{\theta}_T$, which can be optimized to reduce the model variance [42] and thus improve the convergence rate.

We next establish a finite-sample bound on the error, given by the expected loss in the objective value at iteration T with respect to F^* , for both the weighted average model $\hat{\theta}_T$ and instantaneous weights θ_T . We begin with the bound relevant for the average model, stated in the following theorem:

Theorem 1. *Let $\{\theta_t^n\}_{n=1}^N$ be the model parameters generated by COTAF according to (8), and (13) over R rounds, i.e., $t \in \{0, 1, \dots, T-1\}$ with $T = RH$. Then, when *AS1-**

AS3 hold and the step sizes are set to $\eta_t = \frac{4}{\mu(a+t)}$ with shift parameter $a > \max\{16\frac{L}{\mu}, H\}$, and the precoder is set as in (10), it holds that

$$\mathbb{E}[F(\hat{\theta}_T)] - F^* \leq \frac{4(T+R)}{3\mu S_R} (2a+H+R-1)B + \frac{16dT HG^2 \sigma_w^2}{3\mu P N^2 S_R} (2a+T+H) + \frac{\mu a^3}{6S_R} \|\theta_0 - \theta^*\|^2, \quad (15)$$

where $\hat{\theta}_T = \frac{1}{S_R} \sum_{r=1}^R \beta_r \theta_{rH}$, for $\beta_t = (a+t)^2$, $S_R = \sum_{r=1}^R \beta_{rH} \geq \frac{1}{3H} T^3$, and

$$B = 8H^2 G^2 + \frac{1}{N^2} \sum_{n=1}^N M_n^2 + 6L\Gamma. \quad (16)$$

Proof: The proof is given in Appendix A. ■

The weighted average in $\hat{\theta}_T$ is taken over the models known to the server, i.e., $\{\theta_r\}$ with $r \in \mathcal{H}$. For comparison, in previous convergence studies of local SGD and its variants [36], [37], the weighted average is computed over every past model, including those available only to users and not to the server. In such cases, the resulting bound does not necessarily correspond to an actual model used for inference, since the weighted average is not attainable. Comparing Theorem 1 to the corresponding result in [36], which considered i.i.d data and noise-free channels, we observe that COTAF achieves the same convergence rate, with an additional term which depends on the noise-to-signal ratio σ_w^2/P , and decays as $1/T$ as discussed in the sequel. When $\sigma_w^2/P = 0$, Theorem 1 specializes into [36, Thm 2.2].

In the next theorem, we establish a finite sample bound on the error for the instantaneous weights θ_T rather than the weighted average $\hat{\theta}_T$:

Theorem 2. *Let $\{\theta_t^n\}_{n=1}^N$ be the model parameters generated by COTAF according to (8) and (13) over R rounds, i.e., $t \in \{0, 1, \dots, T-1\}$ with $T = RH$. Then, when *AS1-AS3* hold and the step sizes are set to $\eta_t = \frac{2}{\mu(\gamma+t)}$, for $\gamma \geq \max(\frac{8L\rho}{\mu}, H)$, it holds that:*

$$\mathbb{E}[F(\theta_T)] - F(\theta^*) \leq \frac{2L \max(4C, \mu^2 \gamma \delta_0)}{\mu^2 (T + \gamma)}. \quad (17)$$

where $C = B + \frac{4dH^2 G^2 \sigma_w^2}{PN^2}$.

Proof: The proof is given in Appendix B. ■

The proofs for both Theorems 1-2 follow the same first steps. Yet in the derivation of Theorem 2 an additional relaxation was applied, implying that the bound in (17) is less tight than (15). For the noise-free case, i.e., $\sigma_w^2/P = 0$, Theorem 2 coincides with [11, Thm. 1].

Theorems 1 and 2 characterize of the effect of three sources of error on the rate of convergence: The accuracy of the initial guess initial distance θ_0 ; the effect of statistical heterogeneity encapsulated in Γ , which is linear in B and C ; and the noise-to-signal ratio σ_w^2/P induced by the wireless channel. In particular, in (17) all of these quantities, which potentially degrade the accuracy of the learned global model, contribute to the error bound in a manner proportional to $1/(T + \gamma)$, i.e., which decays as the number of rounds grows. The same observation also holds for (15), in which

the aforementioned terms contribute in a manner that decays at an order proportional to $1/T$. The fact that the error due to the noise, encapsulated in σ_w^2/P , decays with the number of iterations, indicates the ability of COTAF to mitigate the harmful effect of the MAC noise, as discussed next.

Comparing (17) to the corresponding bound for local SGD with heterogeneous data and without communication constraints in [11, Thm. 1], i.e., over orthogonal channels as in (6) without noise, we observe that the bound takes a similar form as that in [11, Eq. (5)]. The main difference is in the additional term that depends on the noise-to-signal ratio σ_w^2/P in the constant C , which does not appear in the noiseless case in [11]. Consequently, the fact that COTAF communicates over a noisy channel induces an additional term that can be written as σ_w^2/P times some factor which, as the number of FL rounds R grows, is dominated by $\frac{H^2}{N^2(T+\gamma)}$. This implies that the time-varying precoding and aggregation strategy implemented by COTAF results in a gradual decay of the noise effect, and allows its contribution to be further mitigated by increasing the number of users N . Furthermore, Theorems 1-2 yield the same asymptotic convergence rate to that observed for noiseless local SGD in [11], as stated in the following corollary:

Corollary 1. *COTAF achieves an asymptotic convergence rate of $\mathcal{O}(\frac{1}{T})$.*

Proof: The corollary follows directly from (15) and (17) by letting T grow arbitrarily large while keeping the number of SGD iterations per round H fixed. \square

Corollary 1 implies that COTAF allows OTA FL to achieve the same asymptotic convergence rate as local SGD with a strongly convex objective and without communication constraints [11], [36]. This advantage of COTAF adds to its ability to exploit the temporal and spectral resources of the wireless channel, allowing communication at higher throughput compared to conventional designs based on orthogonal communications, as discussed in Subsection III-D.

C. Extension to Fading Channels

In the previous subsections we focused on FL over wireless channels modeled as noisy MACs (4). For such channels we derived COTAF and characterized its convergence profile. We next show how COTAF can be extended to fading MACs of the form (7), while preserving its proven convergence. As detailed in Subsection II-B, we focus on scenarios in which the participating entities have CSI.

In fading MACs, the signal transmitted by each user undergoes a fading coefficient denoted $h_t^n e^{j\phi_t^n}$ (7). Following the scheme proposed in [18] for conveying sparse model updates, each user can utilize its CSI to cancel the fading effect by amplifying the signal by its inverse channel coefficient. However, weak channels might cause an arbitrarily high amplification, possibly violating the transmission power constraint (5). Therefore, a threshold h_{min} is set, and users observing fading coefficients of a lesser magnitude than h_{min} do not transmit in that communication round. As channels typically attenuate their signals, it holds that

$h_{min} < 1$. Under this extension of COTAF, (9) becomes

$$\mathbf{x}_t^n = \begin{cases} \frac{\sqrt{\alpha_t} h_{min}}{h_t^n} e^{-j\phi_t^n} (\boldsymbol{\theta}_t^n - \boldsymbol{\theta}_{t-H}^n), & h_t^n > h_{min}, \\ 0, & h_t^n \leq h_{min}. \end{cases} \quad (18)$$

Here, $e^{-j\phi_t^n}$ is a phase correction term as in [19]. Note that the energy constraint (5) is preserved as $\mathbb{E}[\|\mathbf{x}_t^n\|^2] \leq P$.

To formulate the server aggregation, we let $\mathcal{K}_t \subset \mathcal{N}$ be the set of user indices whose corresponding channel at time t satisfies $h_t^n > h_{min}$. As the server has CSI, it knows \mathcal{K}_t , and can thus recover the aggregated model $\boldsymbol{\theta}_t$ in a similar manner as in (12)-(13) via $\boldsymbol{\theta}_t = \frac{\mathbf{y}_t}{|\mathcal{K}_t| \sqrt{\alpha_t} h_{min}} + \boldsymbol{\theta}_{t-H}$, i.e.,

$$\boldsymbol{\theta}_t = \frac{1}{|\mathcal{K}_t|} \sum_{n \in \mathcal{K}_t} \boldsymbol{\theta}_t^n + \frac{N}{|\mathcal{K}_t| h_{min}} \mathbf{w}_t. \quad (19)$$

Comparing (19) to the corresponding equivalent formulation in (13), we note that the proposed extension of COTAF results in two main differences from the fading-free scenario: 1) the presence of fading is translated into an increase in the noise power, encapsulated in the constant $\frac{N}{|\mathcal{K}_t| h_{min}} > 1$; and 2) less models are aggregated in each round as $|\mathcal{K}_t| \leq N$. The set of participating users \mathcal{K}_t depends on the distribution of the fading coefficients. Thus, in order to analytically characterize how the convergence is affected by fading compared to the scenario analyzed in Subsection III-B, we introduce the following assumption:

AS4 At each communication round, the participating users set \mathcal{K}_t contains $K \leq N$ users and is uniformly distributed over all the subsets of \mathcal{N} of cardinality K .

Note that Assumption AS4 can be imposed by a simple distributed mechanism using an opportunistic carrier sensing [43]. Specifically, each user maps its h_t^n to a backoff time b_t^n based on a predetermined common function $f(h)$, which is a decreasing function with h (truncated at h_{min}). Then, each user with $h_t^n \geq h_{min}$ listens to the channel and transmits a low-power beacon when its backoff time expires, which can be sensed by other users. If K transmissions have been identified, the corresponding K users transmit their data signal to the server. Otherwise, the users wait (which occurs with a small probability as N increases, and h_{min} decreases) to the next time step. This mechanism guarantees $|\mathcal{K}_t| = K$ at each update. We point out that Assumption AS4 is needed for theoretical analysis only. In practice, COTAF achieves a similar convergence property when implementing it without this mechanism, i.e., when $|\mathcal{K}_t|$ is random.

Next, we characterize the convergence of the instantaneous global model, as stated in the following theorem:

Theorem 3. *Let $\{\boldsymbol{\theta}_t^n\}_{n=1}^N$ be the model parameters generated by the extension of COTAF to fading channels over R rounds, i.e., $t \in \{0, 1, \dots, T-1\}$ with $T = RH$. Then, when AS1-AS4 hold and the step sizes are set to $\eta_t = \frac{2}{\mu(\gamma+t)}$, for $\gamma \geq \max(\frac{8L\rho}{\mu}, H)$, it holds that:*

$$\mathbb{E}[F(\boldsymbol{\theta}_T)] - F(\boldsymbol{\theta}^*) \leq \frac{2L \max(4(\tilde{C} + D), \mu^2 \gamma \delta_0)}{\mu^2(T + \gamma)}. \quad (20)$$

where $\tilde{C} = B + \frac{4dH^2G^2\sigma_w^2}{PK^2h_{min}^2}$ and $D = \frac{4(N-K)}{K(N-1)}H^2G^2$.

Proof: The proof is given in Appendix C. \blacksquare

Comparing Theorem 3 to the corresponding convergence bound for fading-free channels in Theorem 3 reveals that the extension of COTAF allows the trained model to maintain its asymptotic convergence rate of $O(\frac{1}{T})$ also in the presence of fading channel conditions. However, the aforementioned differences in the equivalent global model due to fading are translated here into additive terms increasing the bound on the distance between the expected instantaneous objective $\mathbb{E}[F(\theta_T)]$ and its desired optimal value. In particular, the fact that not all users participate in each round induces the additional positive term D in (20), which equals zero when $K = N$ and grows as K decreases. Furthermore, the increased equivalent noise results in the additive term \tilde{C} in (10), while maintaining the convergence guarantees of Theorems 1-2. Alternatively, since α_t should be proportional to the inverse of the maximal difference of consecutively transmitted models, one can numerically estimate these values by performing offline simulation over a smaller data set. Once these values are numerically computed, the server can distribute them to the users over the downlink channel.

D. Discussion

COTAF is designed to allow FL systems operating over shared wireless channels to exploit the full spectral and temporal resources of the media. This is achieved by accounting for the task of aggregating the local models into a global one as a form of OTA computation [22]. Unlike conventional orthogonality-based transmissions, such as FDM and TDM, in OTA FL the available band and/or transmission time of each user does not decrease with the number of users N , allowing the simultaneous participation of a large number of users without limiting the throughput of each user. Compared to previous strategies for OTA FL, COTAF allows the implementation of local SGD, which is arguably the most widely used FL scheme, over wireless MACs with proven convergence. This is achieved without having to restrict the model updates to be sparse with an identical sparsity pattern shared among all users [17], [18], or requiring the users to repeatedly compute the gradients over the full data set as in [19].

A major challenge in implementing SGD as an OTA computation stems from the presence of the additive channel noise, whose contribution does not decay over time [35]. Under strongly convex objectives, noisy distributed learning can be typically shown to asymptotically converge to some distance from the minimal achievable loss, unlike noise-free local SGD which is known to converge to desired F^* at a rate of $\mathcal{O}(\frac{1}{T})$ [36]. COTAF involves additional precoding and scaling steps which result in an effective decay of the noise contribution, thus allowing to achieve convergence results similar to noise-free local SGD with strongly convex objectives while operating over shared noisy wireless channels. The fact that COTAF mitigates the effect of noise in a gradual manner allows benefiting from the advantages of such noise profiles under non-convex objectives, where a controllable noise level was shown to facilitate convergence by reducing the probability of the learning

procedure being trapped in local minima [39], [41]. This behavior is numerically demonstrated in Section IV.

COTAF consists of an addition of simple precoding and scaling stages to local SGD. This precoding stage is necessary for assuring a steady convergence rate, while keeping power consumption under control. Implementing the time-varying precoding in (10) implies that every user has to know $\max_n \mathbb{E}[\|\theta_t^n - \theta_{t-H}^n\|^2]$, for each communication round $t \in \mathcal{H}$. When operating with a decaying step size, as is commonly required in FL, and when AS3 holds, this term is upper bounded by $H^2 \eta_{t-H}^2 G^2$ (see Lemma A.2 in Appendix A), and the upper bound can be used instead of Theorems 1-2. Alternatively, since α_t should be proportional to the inverse of the maximal difference of consecutively transmitted models, one can numerically estimate these values by performing offline simulation over a smaller data set. Once these values are numerically computed, the server can distribute them to the users over the downlink channel.

COTAF involves analog transmissions over MAC, which allows the superposition carried out by the MAC to aggregate the parameters as required in FL. As a result, COTAF is subject to the challenges associated with such signalling, e.g., the need for accurate synchronization among all users. Finally, OTA FL schemes such as COTAF require the participating users to share the same wireless channel, i.e., reside in the same geographical area, while FL systems can be trained using data aggregated from various locations. We conjecture that COTAF can be combined in multi-stage FL, such as clustered FL [7]. We leave this for future study.

IV. NUMERICAL EVALUATIONS

In this section, we provide numerical examples to illustrate the performance of COTAF in two different settings. We begin with a scenario of learning a linear predictor of the release year of a song from audio features in Subsection IV-A. In this setup, the objective is strongly convex, and the model assumptions under which COTAF is analyzed hold. In the second setting detailed in Subsection IV-B, we consider a more involved setup, in which the loss surface with respect to the learned weights is not convex. Specifically, we train a CNN for classification on the CIFAR-10 dataset.

A. Linear Predictor Using the Million Song Dataset

We start by examining COTAF for learning how to predict the release year of a song from audio features in an FL manner. We use the dataset available by the UCI Machine Learning Repository [44], extracted from the Million Song Dataset collaborative project between The Echo Nest and LabROSA [38]. The Million Song Dataset contains songs which are mostly western, commercial tracks ranging from 1922 to 2011. Each song is associated with a release year and 90 audio attributes. Consequently, each data sample s takes the form $s = \{s_s, s_y\}$, where s_s is the audio attributes vector and s_y is the year. The system task is to train a linear estimator θ with $d = 90$ entries in an FL manner using data available at N users, where each user has access to $D_n = 9200$ samples. The predictor is trained using the regularized linear least-squares loss, given by:

$$f(\theta, \{s_s, s_y\}) = \frac{1}{2}(s_s^T \theta - s_y)^2 + \frac{\lambda}{2} \|\theta\|^2, \quad (21)$$

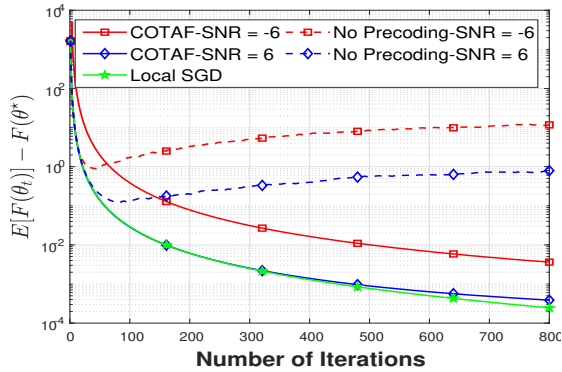


Fig. 3. Linear predictor, Million Song dataset, $H = 40$, $N = 50$.

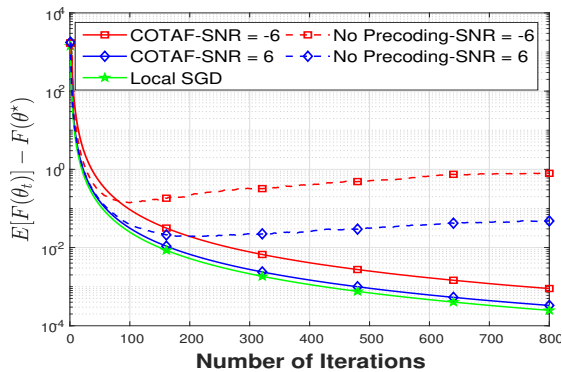


Fig. 4. Linear predictor, Million Song dataset, $H = 40$, $N = 200$. where we used $\lambda = 0.5$. We note that the loss measure (21) is strongly convex and has a Lipschitz gradient, and thus satisfies the conditions of Theorem 1. In every FL round, each user performs H SGD steps (8) where the step size is set via Theorem 1. In particular, the parameters L and μ are numerically evaluated before transmitting the model update to the server over the MAC. The precoding coefficient α_t is computed via (10) using numerical averaging, i.e., we carried out an offline simulation of local SGD without noise and with 20% of the data samples, and computed the averaged norm of the resulting model updates.

We numerically evaluate the gap from the achieved expected objective and the loss-minimizing one, i.e., $\mathbb{E}[F(\theta_t)] - F^*$. Using this performance measure, we compare COTAF to the following FL methods: (i) Local SGD, in which every user conveys its model updates over a noiseless individual channel; (ii) Non-precoded OTA FL, where every user transmits its model updates over the MAC without time-varying precoding (10) and with a constant amplification as in [19], i.e., $\mathbf{x}_t^n = P(\theta_t^n - \theta_{t-H}^n)$. The stochastic expectation is evaluated by averaging over 50 Monte Carlo trials, where in each trial the initial θ_0 is randomized from zero-mean Gaussian distribution with covariance $5\mathbf{I}_d$.

We simulate MACs with signal-to-noise ratios (SNRs) of $P/\sigma_w^2 = -6\text{dB}$ and $P/\sigma_w^2 = 6\text{dB}$. In Fig. 3, we present the performance evaluation when the number of users is set to $N = 50$ and the number of SGD steps is $H = 40$. It can be seen in Fig. 3 that COTAF achieves performance within a minor gap from that of local SGD carried out over ideal orthogonal noiseless channels. This improved performance of COTAF is achieved without requiring the users to divide the spectral and temporal channel resources among each

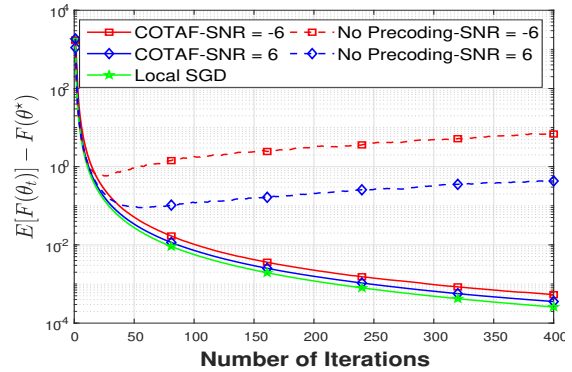


Fig. 5. Linear predictor, Million Song dataset, $H = 80$, $N = 50$.

other, thus to communicate at higher throughput uplink communications as compared to the local SGD. This is due to the precoding scheme of COTAF, which allows gradually mitigating the effect of channel noise, while OTA FL without such time-varying precoding results in a dominant error floor due to presence of non-vanishing noise.

Next, we repeat the simulation study of Fig. 3 while increasing the number of users to be $N = 200$ in Fig. 4, and with setting the number of SGD steps to $H = 80$ in Fig. 5. The number of gradient computations $T = RH$ and the overall number of training samples ND_n is kept constant throughout the simulations. Figs. 4-5 thus demonstrate the dependence of COTAF performance on two key system parameters: The number of users, N , and the number of SGD steps, H , between communication rounds.

Observing Fig. 4 and comparing it to Fig. 3, we note that increasing the number of users improves the performance of both OTA FL schemes, despite the fact that each user holds less training samples. In particular, COTAF effectively coincides with the performance of noise-free local SGD here, while the non-precoded OTA FL achieves an improved performance as compared to the setting with $N = 50$, yet it is still notably outperformed by COTAF. The gain in increasing the number of users follows from the fact that averaging over a larger number of users at the server side mitigates the contribution of the channel noise, as theoretically established for COTAF in Subsection III-B. It is emphasized that when using orthogonal transmissions, as implicitly assumed when using conventional local SGD, increasing the number of users implies that the channel resources must be shared among more users, hence the throughput of each users decreases. However, in OTA FL the throughput is invariant of the number of users. Comparing Fig. 5 to Fig. 3 reveals that increasing the SGD steps H can improve the performance of OTA FL as the channel noise is induced less frequently. Nonetheless, the gains here are far less dominant than those achievable by allowing more users to participate in the FL procedure, as observed in Fig. 4. The results depicted in Figs. 3-5 demonstrate the benefits of COTAF, as an OTA FL scheme which accounts for both the convergence properties of local SGD as well as the unique characteristics of wireless communication channels.

Next, we simulate the effect of fading channels on COTAF. In particular, we apply the extension of COTAF to fading channels detailed in Subsection III-C. Here, the MAC input-output relationship is given by (7), and block fading

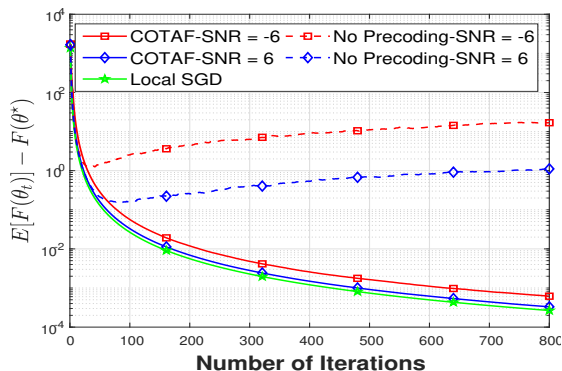


Fig. 6. Linear predictor, Million Song dataset, $H = 40$, $N = 50$, Rayleigh fading channels.

channel coefficients $\{h_t^n\}$ are sampled from a Rayleigh distribution in an i.i.d. fashion, while the remaining parameters are the same as those used in the scenario simulated in Fig. 3. The threshold h_{min} in (18) is set such that on average 40 out of the $N = 50$ users participate in each communication round.

For fairness, the same conditions are applied in the no precoding setting, i.e., the users utilize their CSI to cancel the effect of the channel as in [18]. This comparison allows us to illustrate the significance of the dedicated precoding introduced by COTAF.

The results, depicted in Fig. 6, demonstrate that COTAF maintains its ability to approach the performance of noise-free local SGD, observed in Figs. 3-5 for additive noise MACs. This demonstrates the ability the extended COTAF detailed in Subsection III-C to preserve its improved convergence properties in fading channels.

B. CNN Classifier Using the CIFAR-10 Dataset

Next, we consider an image classification problem, based on the CIFAR-10 dataset, which contains train and test images from ten different categories. The classifier model is the DNN architecture detailed in [45], which consists of three conventional layers and two fully-connected layers. When trained in a centralized setting, this architecture achieves an accuracy of roughly 70% [45]. Here, we train this network to minimize the empirical cross-entropy loss in an FL manner, where the data set is distributed among $N = 10$ users. Each user holds 5000 images, and carries out its local training with a minibatch size of 60 images, while aggregation is done every $H = 84$ iterations over a MAC with SNR of -4 dB. We consider two divisions of the training data among the users: *i.i.d. data*, where we split the data between the users in an i.i.d. fashion, i.e. each user holds the same amount of figures from each class; and *heterogeneous data*, where approximately 20% of the training data of each user is associated with a single label, which differs among the different users. This division causes heterogeneity between the users, as each user holds more images from a unique class. The model accuracy versus the transmission round achieved for the considered FL schemes is depicted in Figs. 7-8 for the i.i.d. case and the heterogeneous case, respectively.

Observing Figs. 7-8, we note that the global model trained using COTAF converges to an accuracy of approximately

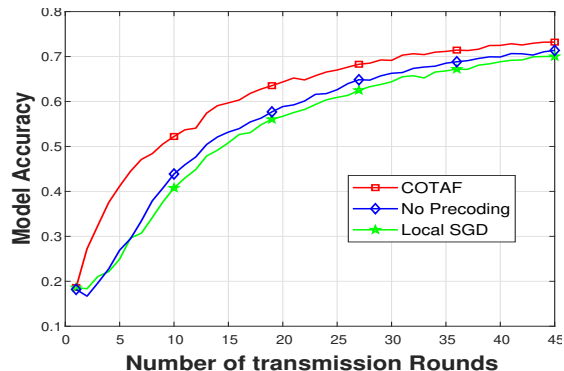


Fig. 7. CNN, CIFAR-10 dataset, i.i.d. data.

70%, i.e., that of the centralized setting. This is achieved while allowing each user to fully utilize its available temporal and spectral channel resources, thus communicating at higher throughput as compared to orthogonal transmissions. Furthermore, we point out the following advantages of COTAF when applied to CIFAR-10:

1) *COTAF achieves the desired sublinear convergence rate:* While the objective in training the CNN to minimize the cross-entropy loss is not a convex function of the weights, we observe the same rate of convergence for COTAF as that of noise-free local SGD. This result suggests a generalization of the theoretical analysis for the convex case and indicates that even in cases in which assumptions *AS1-AS3* do not hold, COTAF is still able to converge in a sub-linear rate. We deduce that COTAF can be applied in settings less restrictive than the analysed case introduced in Subsection III-B and still achieve good results, as numerically illustrated in the current study.

2) *COTAF benefits from the presence of noise:* The simulation results indicate that the additive noise caused by the channel improves the convergence rate and generalization of the CNN model. The fact that COTAF gradually mitigates the effective noise allows it to benefit from its presence in non-convex settings, while notably outperforming direct OTA FL with no time-varying precoding operating in the same channel. Specifically, the presence of noise when training DNNs is known to have positive effects such as reducing overfitting and avoiding local minima. Furthermore, we notice that for the heterogeneous data case in Fig. 8, the gap between COTAF and local SGD is increased as compared to the i.i.d. case in Fig. 7. This indicates that the noise has a smoothing effect as well. It allows better generalizations in the non-i.i.d. setting, which are exploited by COTAF in a manner that contributes to its accuracy more effectively as compared to OTA FL with no precoding.

V. CONCLUSIONS

In this work we proposed the COTAF algorithm for implementing FL over wireless MACs. COTAF maintains the convergence properties of local SGD with heterogeneous data across users, with convex objectives carried out over ideal channels, without requiring the users to divide the channel resources. This is achieved by introducing a time-varying precoding and scaling scheme which facilitates the aggregation and gradually mitigates the noise effect. We prove that for convex objectives, models trained using COTAF with heterogeneous data converge to the loss minimizing model

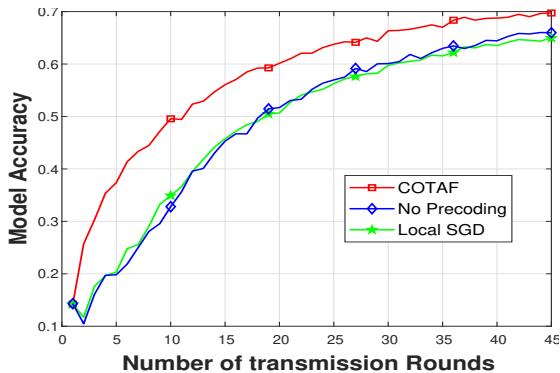


Fig. 8. CNN, CIFAR-10 dataset, heterogeneous data.

with the same asymptotic convergence rate of local SGD over orthogonal channels. Our numerical study demonstrates the ability of COTAF to learn accurate models in over wireless channels using non-synthetic datasets. Furthermore, the simulation results show that COTAF converges in non-convex settings in a sub-linear rate as well, and outperforms not only OTA FL without precoding, but also the local SGD algorithm in an orthogonal fashion without errors.

APPENDIX

A. Proof of Theorem 1

In the following, we detail the proof of Theorem 1, introduced in Subsection III-B. The intermediate derivations detailed below are used in proving Theorem 2 in Appendix B as well. The outline of the proof is as follows: First, we define a virtual sequence $\{\bar{\theta}_t\}$ that represents the averaged parameters over all users at every iteration in (A.1), i.e. as if the local SGD framework is replaced with mini-batch SGD. While $\bar{\theta}_t$ can not be explicitly computed at each time instance by any of the users or the server, it facilitates utilizing bounds established for mini-batch SGD, as was done in [11], [36]. Next, we provide in Lemma A.1 a single step recursive bound for the error $E[\|\bar{\theta}_t - \theta^*\|^2]$. The bound consists four terms, and so, in Lemmas A.2 and A.3 we upper bound these quantities. Finally, we obtain a non-recursive bound from the recursive expression in Lemma A.4, with which we prove Theorem 1.

Recursive error formulation: Following the steps used in the corresponding convergence analysis of FL without communication constraints [11], [36], we first define the virtual sequence $\{\bar{\theta}_t\}_{t \geq 0}$. Broadly speaking, $\{\bar{\theta}_t\}$ represents the weights obtained when the weights trained by the users are aggregated and averaged over the true channel on each H SGD steps, and over a virtual noiseless channel on the remaining SGD iterations. This virtual sequence is given by

$$\bar{\theta}_t \triangleq \frac{1}{N} \sum_{n=1}^N \theta_t^n + \frac{1}{\sqrt{\alpha_t N}} \bar{\mathbf{w}}_t \mathbb{1}_{t \in \mathcal{H}}, \quad (\text{A.1})$$

where $\mathbb{1}(\cdot)$ is the indicator function. Rearranging (A.1) to fit our transmission scheme yields:

$$\bar{\theta}_t = \bar{\theta}_{t-H} + \frac{1}{\sqrt{\alpha_t N}} \sum_{n=1}^N \sqrt{\alpha_t} (\theta_t^n - \bar{\theta}_{t-H}) + \mathbf{w}_t \mathbb{1}_{t \in \mathcal{H}}, \quad (\text{A.2})$$

with $\bar{\theta}_t \triangleq \theta_0$ for $t \leq 0$. The scaled noise $\mathbf{w}_t = \frac{1}{\sqrt{\alpha_t N}} \bar{\mathbf{w}}_t$, and the sequence $\{\theta_t^n\}_{t \geq 0}$ are defined in Subsection III-A.

Notice that $\{\bar{\theta}_t\}$ is not computed explicitly, and that $\bar{\theta}_t = \theta_t^n$ for each $n \in \mathcal{N}$ whenever $t \in \mathcal{H}$. We also define

$$\mathbf{g}_t \triangleq \frac{1}{N} \sum_{n=1}^N \nabla f_{i_t^n}(\theta_t^n), \quad \bar{\mathbf{g}}_t \triangleq \frac{1}{N} \sum_{n=1}^N \nabla F(\theta_t^n). \quad (\text{A.3})$$

Since the indices i_t^n used in each SGD iteration are uniformly distributed, it follows that $\mathbb{E}[\mathbf{g}_t] = \bar{\mathbf{g}}_t$. By writing $\bar{\mathbf{w}}_t \triangleq \mathbf{w}_{t+1} \mathbb{1}_{t+1 \in \mathcal{H}} - \mathbf{w}_t \mathbb{1}_{t \in \mathcal{H}}$, we have that

$$\bar{\theta}_{t+1} = \bar{\theta}_t - \eta_t \mathbf{g}_t + \bar{\mathbf{w}}_t. \quad (\text{A.4})$$

The equivalent noise vector $\bar{\mathbf{w}}_t$ is zero-mean and satisfies

$$\begin{aligned} \mathbb{E}[\|\bar{\mathbf{w}}_t\|^2] &= \frac{d\sigma_w^2}{N^2} \left(\frac{1}{\alpha_{t+1}} \mathbb{1}_{t+1 \in \mathcal{H}} + \frac{1}{\alpha_t} \mathbb{1}_{t \in \mathcal{H}} \right) \\ &\leq \frac{d\sigma_w^2}{N^2 \min(\alpha_t, \alpha_{t+1})} \mathbb{I}_t, \end{aligned} \quad (\text{A.5})$$

where $\mathbb{I}_t \triangleq \mathbb{1}_{(t \in \mathcal{H}) \cup (t+1 \in \mathcal{H})}$. Theorem 1 is obtained from definitions (A.1) and (A.3) via the following lemma:

Lemma A.1. *Let $\{\theta_t^n\}$ and $\{\bar{\theta}_t\}$ be as defined in (14) and (A.1), respectively. Then, when AS1-AS2 are satisfied and the SGD step size satisfies $\eta_t \leq \frac{1}{4L}$, it holds that*

$$\begin{aligned} \mathbb{E}[\|\bar{\theta}_{t+1} - \theta^*\|^2] &\leq (1 - \mu\eta_t) \mathbb{E}[\|\bar{\theta}_t - \theta^*\|^2] \\ &\quad + \eta_t^2 \mathbb{E}\left[\left\|\mathbf{g}_t - \bar{\mathbf{g}}_t + \frac{\bar{\mathbf{w}}_t}{\eta_t}\right\|^2\right] - \frac{3}{2} \eta_t \mathbb{E}[F(\bar{\theta}_t) - F^*] \\ &\quad + \frac{2}{N} \sum_{n=1}^N \mathbb{E}[\|\bar{\theta}_t - \theta_t^n\|^2] + 6L\eta_t^2 \Gamma. \end{aligned} \quad (\text{A.6})$$

Proof. Using the update rule we have:

$$\begin{aligned} \|\bar{\theta}_{t+1} - \theta^*\|^2 &= \|\bar{\theta}_t - \eta_t \mathbf{g}_t - \theta^* + \bar{\mathbf{w}}_t\|^2 \\ &= \|\bar{\theta}_t - \eta_t \mathbf{g}_t - \theta^* - \eta_t \bar{\mathbf{g}}_t + \eta_t \bar{\mathbf{g}}_t + \bar{\mathbf{w}}_t\|^2 \\ &= \|\bar{\theta}_t - \eta_t \bar{\mathbf{g}}_t - \theta^*\|^2 + \eta_t^2 \left\| \bar{\mathbf{g}}_t - \mathbf{g}_t + \frac{\bar{\mathbf{w}}_t}{\eta_t} \right\|^2 \\ &\quad + 2\eta_t \left\langle \bar{\theta}_t - \theta^* - \eta_t \bar{\mathbf{g}}_t, \bar{\mathbf{g}}_t - \mathbf{g}_t + \frac{\bar{\mathbf{w}}_t}{\eta_t} \right\rangle. \end{aligned} \quad (\text{A.7})$$

Observe that $E[\langle \bar{\theta}_t - \theta^* - \eta_t \bar{\mathbf{g}}_t, \bar{\mathbf{g}}_t - \mathbf{g}_t + \frac{\bar{\mathbf{w}}_t}{\eta_t} \rangle] = 0$. Following the proof steps in [11, Lemma 1], we obtain

$$\begin{aligned} \|\bar{\theta}_t - \eta_t \bar{\mathbf{g}}_t - \theta^*\|^2 &\leq (1 - \mu\eta_t) \|\bar{\theta}_t - \theta^*\|^2 + \frac{1}{N} \sum_{n=1}^N \|\bar{\theta}_t - \theta_t^n\|^2 \\ &\quad + \underbrace{\frac{4L\eta_t^2}{N} \sum_{n=1}^N (f_n(\theta_t^n) - f_n^*) - \frac{2\eta_t}{N} \sum_{n=1}^N f_n(\theta_t^n) - f_n(\theta^*)}_{\triangleq A}. \end{aligned}$$

Observe that A defined above satisfies:

$$\begin{aligned} A &= \frac{1}{N} \sum_{n=1}^N [(4L\eta_t^2 - 2\eta_t) f_n(\theta_t^n) - 4L\eta_t^2 f_n^* + 2\eta_t f_n(\theta^*)] \\ &\stackrel{(a)}{=} \frac{4L\eta_t^2 - 2\eta_t}{N} \sum_{n=1}^N (f_n(\theta_t^n) - F^*) + \frac{4L\eta_t^2}{N} \sum_{n=1}^N (F^* - f_n^*) \\ &\stackrel{(b)}{=} (4L\eta_t^2 - 2\eta_t) \frac{1}{N} \sum_{n=1}^N (f_n(\theta_t^n) - F^*) + 4L\eta_t^2 \Gamma, \end{aligned} \quad (\text{A.8})$$

where (a) and (b) follow from the definitions of F^* and Γ ,

respectively. Notice that $4L\eta_t^2 - 2\eta_t \leq \eta_t - 2\eta_t \leq -\eta_t$.

Next, we use the following inequality obtained in [11]

$$\begin{aligned} \frac{1}{N} \sum_{n=1}^N (f_n(\boldsymbol{\theta}_t^n) - F^*) &\geq (F(\bar{\boldsymbol{\theta}}_t) - F^*) \\ &- \frac{1}{N} \sum_{n=1}^N \left[\eta_t L(f_n(\bar{\boldsymbol{\theta}}_t) - f_n^*) + \frac{1}{2\eta_t} \|\boldsymbol{\theta}_t^n - \bar{\boldsymbol{\theta}}_t\|^2 \right]. \end{aligned} \quad (\text{A.9})$$

Substituting (A.9) into (A.8) yields:

$$\begin{aligned} A &\leq \frac{2\eta_t - 4L\eta_t^2}{N} \sum_{n=1}^N \left[\eta_t L(f_n(\bar{\boldsymbol{\theta}}_t) - f_n^*) + \frac{1}{2\eta_t} \|\boldsymbol{\theta}_t^n - \bar{\boldsymbol{\theta}}_t\|^2 \right] \\ &\quad - (2\eta_t - 4L\eta_t^2)(F(\bar{\boldsymbol{\theta}}_t) - F^*) + 4L\eta_t^2 \Gamma \\ &= (2\eta_t - 4L\eta_t^2)(\eta_t L - 1)(F(\bar{\boldsymbol{\theta}}_t) - F^*) \\ &\quad + ((2\eta_t - 4L\eta_t^2)\eta_t + 4\eta_t^2)L\Gamma + \frac{(2\eta_t - 4L\eta_t^2)}{2\eta_t N} \sum_{n=1}^N \|\boldsymbol{\theta}_t^n - \bar{\boldsymbol{\theta}}_t\|^2 \\ &\stackrel{(a)}{\leq} 6L\eta_t^2 \Gamma - \frac{3\eta_t}{2} (F(\bar{\boldsymbol{\theta}}_t) - F^*) + \frac{1}{N} \sum_{n=1}^N \|\boldsymbol{\theta}_t^n - \bar{\boldsymbol{\theta}}_t\|^2, \end{aligned} \quad (\text{A.10})$$

where in (a) we use the following facts: (1) $\eta_t L - 1 \leq -\frac{3}{4}$,

(2) $2\eta_t - 4L\eta_t^2 \leq 2\eta_t$. Consequently, we have that:

$$\begin{aligned} \|\bar{\boldsymbol{\theta}}_t - \boldsymbol{\theta}^* - \eta_t \bar{\boldsymbol{g}}_t\|^2 &\leq (1 - \mu\eta_t) \|\bar{\boldsymbol{\theta}}_t - \boldsymbol{\theta}^*\|^2 \\ &+ \frac{2}{N} \sum_{n=1}^N \|\bar{\boldsymbol{\theta}}_t - \boldsymbol{\theta}_t^n\|^2 + 6L\eta_t^2 \Gamma - \frac{3\eta_t}{2} (F(\bar{\boldsymbol{\theta}}_t) - F^*). \end{aligned} \quad (\text{A.11})$$

Finally, by taking the expected value of both sides of (A.7) and using (A.11) we complete the proof. \square

Upper bounds on the additive terms: Next, we prove the theorem by bounding the summands constituting the right hand side of (A.6). First, we bound $\mathbb{E}[\|\boldsymbol{g}_t - \bar{\boldsymbol{g}}_t + \frac{\bar{\boldsymbol{w}}_t}{\eta_t}\|^2]$, as stated in the following lemma:

Lemma A.2. *When the step size sequence $\{\eta_t\}$ consists of decreasing positive numbers satisfying $\eta_t \leq 2\eta_{t+H}$ for all $t \geq 0$ and AS3 holds, then*

$$\mathbb{E}[\|\boldsymbol{g}_t - \bar{\boldsymbol{g}}_t + \frac{\bar{\boldsymbol{w}}_t}{\eta_t}\|^2] \leq \frac{1}{N^2} \sum_{n=1}^N M_n^2 + \frac{4dH^2 G^2 \sigma_w^2}{PN^2} \mathbb{I}_t.$$

Proof. The lemma follows since the noise term $\bar{\boldsymbol{w}}_t$ is zero-mean and independent of the stochastic gradients, hence

$$\begin{aligned} \mathbb{E} \left[\left\| \bar{\boldsymbol{g}}_t - \boldsymbol{g}_t + \frac{\bar{\boldsymbol{w}}_t}{\eta_t} \right\|^2 \right] &= \mathbb{E}[\|\bar{\boldsymbol{g}}_t - \boldsymbol{g}_t\|^2] + \mathbb{E} \left[\left\| \frac{\bar{\boldsymbol{w}}_t}{\eta_t} \right\|^2 \right] \\ &\stackrel{(a)}{\leq} \frac{1}{N^2} \sum_{n=1}^N M_n^2 + \mathbb{E} \left[\left\| \frac{\bar{\boldsymbol{w}}_t}{\eta_t} \right\|^2 \right], \end{aligned} \quad (\text{A.12})$$

where (a) follows from AS3. The first summand in (A.12) coincides with [11, Lemma 2]. From (A.5) we obtain

$$\mathbb{E} \left[\left\| \frac{\bar{\boldsymbol{w}}_t}{\eta_t} \right\|^2 \right] \leq \frac{d\sigma_w^2 \mathbb{I}_t}{\eta_t^2 N^2 \min(\alpha_t, \alpha_{t+1})}. \quad (\text{A.13})$$

Next, we bound $\frac{1}{\alpha_t} = \frac{1}{P} \max_n \mathbb{E}[\|\boldsymbol{\theta}_t^n - \boldsymbol{\theta}_{t-H}^n\|^2]$ via:

$$\begin{aligned} \frac{1}{\alpha_t} &\stackrel{(a)}{\leq} \frac{1}{P} \max_n \left(H\eta_{t-H} \sum_{t'=t-H}^{t-1} \mathbb{E}[\|\nabla f_{i_t^k}(\bar{\boldsymbol{\theta}}_{t'}^n)\|^2] \right) \\ &\stackrel{(b)}{\leq} \frac{1}{P} H^2 \eta_{t-H}^2 G^2 \stackrel{(c)}{\leq} \frac{1}{P} 4H^2 \eta_t^2 G^2, \end{aligned} \quad (\text{A.14})$$

where (a) follows from (8), using the inequality $\|\sum_{t'=t-H}^t \boldsymbol{r}_{t'}\|^2 \leq H \sum_{t'=t-H}^t \|\boldsymbol{r}_{t'}\|^2$, which holds for any multivariate sequence $\{\boldsymbol{r}_t\}$, while noting that the step size is monotonically non-increasing; (b) holds by AS3; and (c) holds as $\eta_t \leq 2\eta_{t+H}$ for all $t \geq 0$. Finally, notice that

$$\begin{aligned} \frac{1}{\min(\alpha_t, \alpha_{t+1})} &= \max \left(\frac{1}{\alpha_t}, \frac{1}{\alpha_{t+1}} \right) \\ &\leq \frac{1}{P} 4H^2 G^2 \max(\eta_t^2, \eta_{t+1}^2) = \frac{1}{P} 4H^2 \eta_t^2 G^2, \end{aligned} \quad (\text{A.15})$$

as $\{\eta_t\}$ is monotonically decreasing. Substituting (A.15) into (A.13) completes the proof. \square

In the next lemma, we bound $\frac{1}{N} \sum_{n=1}^N \mathbb{E}[\|\bar{\boldsymbol{\theta}}_t - \boldsymbol{\theta}_t^n\|^2]$:

Lemma A.3. *When the step size sequence $\{\eta_t\}$ consists of decreasing positive numbers satisfying $\eta_t \leq 2\eta_{t+H}$ for all $t \geq 0$ and AS3 holds, then $\mathbb{E}[\|\bar{\boldsymbol{\theta}}_t - \boldsymbol{\theta}_t^n\|^2] \leq 4\eta_t^2 G^2 H^2$.*

Proof. The lemma follows directly from [36, Lem. 3.3]. \square

Obtaining a non-recursive convergence bound: Combining Lemmas A.1-A.3 yields a recursive relationship which allows us to characterize the convergence of COTAF. To complete the proof, we next establish the convergence bound from the recursive equations, based on the following lemma:

Lemma A.4. *Let $\{\delta_t\}_{t \geq 0}$ and $\{e_t\}_{t \geq 0}$ be two positive sequences satisfying*

$$\delta_{t+1} \leq (1 - \mu\eta_t)\delta_t - \eta_t e_t A + \eta_t^2 B + \eta_t^2 D_t, \quad (\text{A.16})$$

for $\eta_t = \frac{4}{\mu(a+t)}$ with constants $A > 0, B, C \geq 0, \mu > 0, a > 1$ and $D_t = D\mathbb{1}_{t \in \mathcal{H}}$. Then, for any positive integer R it holds that

$$\begin{aligned} \frac{A}{S_R} \sum_{r=1}^R \beta_{rH} e_{rH} &\leq \frac{\mu a^3}{4S_R} \delta_0 + \frac{2R(H+1)}{\mu S_R} B(2a + H + R - 1) \\ &\quad + \frac{2R}{\mu S_R} D(2a + HR + H), \end{aligned} \quad (\text{A.17})$$

for $\beta_t = (a+t)^2$, $T = RH$ and $S_R = \sum_{r=1}^R \beta_{rH} = a^2 R + aT(R+1) + \frac{2T^2 R + T^2 + TH}{6} \geq \frac{1}{3H} T^3 = \frac{1}{3} T^2 R$.

Proof. To prove the lemma, we first note that by [37, Eqn.(45)], it holds that

$$\begin{aligned} (1 - \mu\eta_t) \frac{\beta_t}{\eta_t} &= \left(\frac{a+t-4}{4} \right) \frac{\mu(a+t)^3}{a+t} \\ &= \frac{\mu(a+t-4)(a+t)^2}{4} \\ &\leq \frac{\mu(a+t-1)^3}{4} = \frac{\beta_{t-1}}{\eta_{t-1}}. \end{aligned} \quad (\text{A.18})$$

Therefore, multiplying (A.16) by $\frac{\beta_t}{\eta_t}$ yields

$$\delta_{t+1} \frac{\beta_t}{\eta_t} \leq (1 - \mu\eta_t) \frac{\beta_t}{\eta_t} \delta_t - \beta_t e_t A + \beta_t \eta_t B + \beta_t \eta_t D_t. \quad (\text{A.19})$$

Next, we extract the relations between two sequential rounds, i.e. δ_t, δ_{t+H} . Note that in each round a single D_t is activated, i.e., only a single entry in the set $\{D_\tau\}_{\tau=t}^{t+H}$ is non-zero. Therefore, by repeating the recursion (A.19) over H time instances, we get

$$\begin{aligned} \delta_{t+H} \frac{\beta_{t+H-1}}{\eta_{t+H-1}} &\leq (1 - \mu\eta_t) \frac{\beta_t}{\eta_t} \delta_t - \sum_{\tau=t}^{t+H-1} \beta_\tau e_\tau A \\ &\quad + \sum_{\tau=t}^{t+H-1} \beta_\tau \eta_\tau B + \beta_{t_0} \eta_{t_0} D \\ &\leq (1 - \mu\eta_t) \frac{\beta_t}{\eta_t} \delta_t + \frac{2B}{\mu} (H+1)(H+2t+2a) \\ &\quad - \beta_t e_t A + \beta_{t_0} \eta_{t_0} D, \end{aligned} \quad (\text{A.20})$$

where t_0 is the only time instance in the interval $[t, t+H]$ such that $t_0 \in \mathcal{H}$. In the last inequality we used the fact that $A\beta_t e_t > 0$. Recursively applying (A.20) R times yields:

$$\begin{aligned} \delta_R \frac{\beta_R}{\eta_R} &\leq (1 - \mu\eta_0) \frac{\beta_0}{\eta_0} \delta_0 - \sum_{r=1}^R \beta_{rH} e_{rH} A + \sum_{r=1}^R \beta_{rH} \eta_{rH} D \\ &\quad + \sum_{r=1}^R \frac{2B}{\mu} (H+1)(H+2rH+2a). \end{aligned} \quad (\text{A.21})$$

As $\delta_t \frac{\beta_t}{\eta_t} > 0$ for each t , (A.21) implies that

$$\begin{aligned} A \sum_{r=1}^R \beta_{rH} e_{rH} &\leq \frac{\beta_0}{\eta_0} \delta_0 + \frac{2B(H+1)}{\mu} \sum_{r=1}^R (H+2rH+2a) \\ &\quad + \sum_{r=1}^R \beta_{rH} \eta_{rH} D. \end{aligned} \quad (\text{A.22})$$

Next, recalling that $\beta_t \eta_t = \frac{4(a+t)}{\mu}$, we obtain:

$$\sum_{r=1}^R \beta_{rH} \eta_{rH} D = \frac{4}{\mu} D \left(aR + \frac{HR}{2} + \frac{HR^2}{2} \right). \quad (\text{A.23})$$

For the current setting of β_t and η_t it holds that $\frac{\beta_0}{\eta_0} = \frac{\mu a^3}{4}$. Further, $\sum_{r=1}^R (H+2rH+2a) = R(2a+T+2H)$. Substituting this and (A.23) into the above inequality proves the lemma. \square

We complete the proof of the theorem by combining Lemmas A.1-A.4 as follows: By defining $\delta_t \triangleq \mathbb{E}[\|\bar{\theta}_t - \theta^*\|^2]$, it follows from Lemma A.1 combined with the bounds stated in Lemmas A.2-A.3 that:

$$\begin{aligned} \delta_{t+1} &\leq (1 - \mu\eta_t) \delta_t + \eta_t^2 \left(\frac{1}{N^2} \sum_{n=1}^N M_n^2 + \frac{4dH^2G^2\sigma_w^2}{PN^2} \mathbb{I}_t \right) \\ &\quad - \frac{3}{2} \eta_t \mathbb{E}[F(\bar{\theta}_t) - F^*] + 8\eta_t^2 H^2 G^2 + 6L\eta_t^2 \Gamma. \end{aligned} \quad (\text{A.24})$$

In the non-trivial case where $H > 1$, at most one element of $\{t_0+1, t_0\}$ can be in \mathcal{H} for any t_0 . Therefore, without loss of generality, we reduce the set over which the indicator

function in (A.24) is defined to be $\{t \in \mathcal{H}\}$. By defining

$$\begin{aligned} A &\triangleq \frac{3}{2}; \quad B \triangleq 8H^2G^2 + \frac{1}{N^2} \sum_{n=1}^N M_n^2 + 6L\Gamma; \\ e_t &\triangleq \mathbb{E}[F(\bar{\theta}_t) - F^*]; \quad D_t \triangleq \frac{4dH^2G^2\sigma_w^2}{PN^2} \mathbb{1}_{t \in \mathcal{H}}, \end{aligned}$$

and plugging these notations into Lemma A.4, we obtain

$$\begin{aligned} \frac{1}{S_R} \sum_{r=1}^R \beta_{rH} \mathbb{E}[F(\bar{\theta}_{rH}) - F^*] &\leq \frac{\mu a^3}{6S_R} \|\theta_0 - \theta^*\|^2 \\ &\quad + \frac{4(T+R)}{3\mu S_R} (2a+H+R-1)B + \frac{16dTHG^2\sigma_w^2}{3\mu PN^2 S_R} (2a+T+H). \end{aligned}$$

Finally, by the convexity of the objective function, it holds that

$$\mathbb{E}[F(\hat{\theta}_T) - F^*] \leq \frac{1}{S_R} \sum_{r=1}^R \beta_{rH} \mathbb{E}[F(\bar{\theta}_{rH}) - F^*], \quad (\text{A.25})$$

thus proving Theorem 1. \square

B. Proof of Theorem 2

The proof of Theorem 2 utilizes Lemmas A.1-A.3, stated in Appendix A, while formulating an alternative non-recursive bound compared to that used in Appendix A. To obtain the convergence bound in (17), we first recall the definition $\delta_t \triangleq \mathbb{E}\{\|\bar{\theta}_{t+1} - \theta^*\|^2\}$. When $t \in \mathcal{H}$, the term δ_t represents the ℓ_2 norm of the error in the weights of the global model. We can upper bound (A.24) and formulate the following recursive relationship on the weights error

$$\delta_{t+1} \leq (1 - \eta_t \mu) \delta_t + \eta_t^2 C, \quad (\text{B.1})$$

where $C = B + \frac{4dH^2G^2\sigma_w^2}{PN^2}$. The inequality is obtained from (A.24) since $-\eta_t e_t \mathbb{E}[F(\bar{\theta}_t) - F^*] \leq 0$ and as $D\mathbb{1}_{t \in \mathcal{H}} \leq D$, for $D \geq 0$. The convergence bound is achieved by properly setting the step-size and the FL systems parameters in (B.1) to bound δ_t , and combining the resulting bound with the strong convexity of the objective. In particular, we set the step size η_t to take the form $\eta_t = \frac{\rho}{t+\gamma}$ for some $\rho > \frac{1}{\mu}$ and $\gamma \geq \max(4L\rho, H)$, for which $\eta_t \leq \frac{1}{4L}$ and $\eta_t \leq 2\eta_{t+H}$, implying that Lemmas A.2-A.3 hold.

Under such settings, we show that there exists a finite ν such that $\delta_t \leq \frac{\nu}{t+\gamma}$ for all integer $t \geq 0$. We prove this by induction, noting that setting $\nu \geq \gamma\delta_0$ guarantees that it holds for $t = 0$. We next show that if $\delta_t \leq \frac{\nu}{t+\gamma}$, then $\delta_{t+1} \leq \frac{\nu}{t+1+\gamma}$. It follows from (B.1) that

$$\begin{aligned} \delta_{t+1} &\leq \left(1 - \frac{\rho}{t+\gamma}\mu\right) \frac{\nu}{t+\gamma} + \left(\frac{\rho}{t+\gamma}\right)^2 C \\ &= \frac{1}{t+\gamma} \left(\left(1 - \frac{\rho}{t+\gamma}\mu\right) \nu + \frac{\rho^2}{t+\gamma} C \right). \end{aligned} \quad (\text{B.2})$$

Consequently, $\delta_{t+1} \leq \frac{\nu}{t+1+\gamma}$ holds when

$$\frac{1}{t+\gamma} \left(\left(1 - \frac{\rho}{t+\gamma}\mu\right) \nu + \frac{\rho^2}{t+\gamma} C \right) \leq \frac{\nu}{t+1+\gamma},$$

or, equivalently,

$$\left(1 - \frac{\rho}{t+\gamma}\mu\right) \nu + \frac{\rho^2}{t+\gamma} C \leq \frac{t+\gamma}{t+1+\gamma} \nu. \quad (\text{B.3})$$

By setting $\nu \geq \frac{\rho^2 C}{\rho\mu-1}$, the left hand side of (B.3) satisfies

$$\begin{aligned} \left(1 - \frac{\rho}{t+\gamma}\mu\right)\nu + \frac{\rho^2}{t+\gamma}C &= \frac{t-1+\gamma}{t+\gamma}\nu + \left(\frac{\rho^2}{t+\gamma}C - \frac{\rho\mu-1}{t+\gamma}\nu\right) \\ &= \frac{t-1+\gamma}{t+\gamma}\nu + \frac{\rho^2 C - (\rho\mu-1)\nu}{t+\gamma} \stackrel{(a)}{\leq} \frac{t-1+\gamma}{t+\gamma}\nu, \end{aligned} \quad (\text{B.4})$$

where (a) holds since $\nu \geq \frac{\rho^2 C}{\rho\mu-1}$. As the right hand side of (B.4) is not larger than that of (B.3), it follows that (B.3) holds for the current setting, proving that $\delta_{t+1} \leq \frac{\nu}{t+1+\gamma}$. Finally, the smoothness of the objective implies that

$$\mathbb{E}\{F(\boldsymbol{\theta}_t)\} - F(\boldsymbol{\theta}^*) \leq \frac{L}{2}\delta_t \leq \frac{L\nu}{2(t+\gamma)}, \quad (\text{B.5})$$

which, in light of the above setting, holds for $\nu = \max\left(\frac{\rho^2 C}{\rho\mu-1}, \gamma\delta_0\right)$, $\gamma \geq \max(H, 4\rho L)$, and $\rho > 0$. In particular, setting $\rho = \frac{2}{\mu}$ results in $\gamma = \max(H, 8L/\mu)$, $\nu = \max\left(\frac{4C}{\mu^2}, \gamma\delta_0\right)$ and

$$\mathbb{E}[F(\boldsymbol{\theta}_t)] - F(\boldsymbol{\theta}^*) \leq \frac{2L \max(4C, \mu^2\gamma\delta_0)}{\mu^2(t+\gamma)}, \quad (\text{B.6})$$

thus concluding the proof of Theorem 2. \square

C. Proof of Theorem 3

First, as done in Appendix A, we the virtual sequence $\{\bar{\boldsymbol{\theta}}_t\}$, which here is given by

$$\bar{\boldsymbol{\theta}}_{t+1} = \begin{cases} \frac{1}{N} \sum_{n=1}^N \boldsymbol{\theta}_t^n, & t+1 \notin \mathcal{H}, \\ \frac{1}{K} \sum_{n \in \mathcal{K}_t} \boldsymbol{\theta}_t^n + \frac{N}{Kh_{\min}} \mathbf{w}_t, & t+1 \in \mathcal{H}. \end{cases} \quad (\text{C.1})$$

Let $\bar{\mathbf{v}}_t \triangleq \frac{1}{N} \sum_{n=1}^N \boldsymbol{\theta}_t^n + \frac{N}{Kh_{\min}} \mathbf{w}_t \mathbb{1}_{t \in \mathcal{H}}$ be the virtual sequence of the averaged model over all users. Therefore $\bar{\mathbf{v}}_t = \bar{\boldsymbol{\theta}}_t$ when $t \notin \mathcal{H}$. Under this notation, Theorem 2 characterizes the convergence of $\mathbb{E}[F(\bar{\mathbf{v}}_t)] - F(\boldsymbol{\theta}^*)$. We use the following lemmas, proved in [11, Appendix B.4].

Lemma C.1. *Under assumption AS4 $\bar{\boldsymbol{\theta}}_t$ is an unbiased estimation of $\bar{\mathbf{v}}_t$, i.e. $\mathbb{E}_{\mathcal{K}_t}[\bar{\boldsymbol{\theta}}_t] = \bar{\mathbf{v}}_t$.*

Lemma C.2. *The expected difference between $\bar{\boldsymbol{\theta}}_t$ and $\bar{\mathbf{v}}_t$ is bounded by:*

$$\mathbb{E}_{\mathcal{K}_t}[\|\bar{\mathbf{v}}_t - \bar{\boldsymbol{\theta}}_t\|^2] \leq \frac{4(N-K)}{(N-1)K} \eta_t^2 H^2 G^2. \quad (\text{C.2})$$

We next use these lemmas to prove the theorem, as

$$\begin{aligned} \|\bar{\boldsymbol{\theta}}_{t+1} - \boldsymbol{\theta}^*\|^2 &= \|\bar{\boldsymbol{\theta}}_{t+1} - \bar{\mathbf{v}}_{t+1} + \bar{\mathbf{v}}_{t+1} - \boldsymbol{\theta}^*\|^2 \\ &= \underbrace{\|\bar{\boldsymbol{\theta}}_{t+1} - \bar{\mathbf{v}}_{t+1}\|^2}_{A_1} + \underbrace{\|\bar{\mathbf{v}}_{t+1} - \boldsymbol{\theta}^*\|^2}_{A_2} \\ &\quad + 2 \underbrace{\langle \bar{\boldsymbol{\theta}}_{t+1} - \bar{\mathbf{v}}_{t+1}, \bar{\mathbf{v}}_{t+1} - \boldsymbol{\theta}^* \rangle}_{A_3} \end{aligned} \quad (\text{C.3})$$

The term $\mathbb{E}_{\mathcal{K}_t}[A_3] = 0$ since $\bar{\boldsymbol{\theta}}_t$ is unbiased by Lemma C.1. Further, using Lemma C.2, Theorem 2, and the equivalent global model in (19) to bound A_1 and A_2 respectively:

$$\mathbb{E}[\|\bar{\boldsymbol{\theta}}_{t+1} - \boldsymbol{\theta}^*\|^2] \leq (1 - \eta_t \mu) \mathbb{E}[\|\bar{\boldsymbol{\theta}}_t - \boldsymbol{\theta}^*\|^2] + \eta_t^2 (\tilde{C} + D) \quad (\text{C.4})$$

where $D = \frac{4(N-K)}{K(N-1)} H^2 G^2$. Notice the difference between equations (B.1) and (C.4) is in the additional constant D , and the scaling of the noise-to-signal ratio in \tilde{C} compared to C

in Theorem 2. The same arguments used in proving Theorem 2 can now be applied to (C.4) to prove the theorem. \square

REFERENCES

- [1] T. Sery, N. Shlezinger, K. Cohen, and Y. C. Eldar, "COTAF: Convergent over-the-air federated learning," in *IEEE GLOBECOM*, 2020.
- [2] Y. LeCun, Y. Bengio, and G. Hinton, "Deep learning," *Nature*, vol. 521, no. 7553, p. 436, 2015.
- [3] J. Chen and X. Ran, "Deep learning with edge computing: A review," *Proc. IEEE*, vol. 107, no. 8, pp. 1655–1674, 2019.
- [4] H. B. McMahan, E. Moore, D. Ramage, and S. Hampson, "Communication-efficient learning of deep networks from decentralized data," *arXiv preprint arXiv:1602.05629*, 2016.
- [5] P. Kairouz *et al.*, "Advances and open problems in federated learning," *arXiv preprint arXiv:1912.04977*, 2019.
- [6] V. Smith, C.-K. Chiang, M. Sanjabi, and A. S. Talwalkar, "Federated multi-task learning," in *Proc. NeurIPS*, 2017, pp. 4424–4434.
- [7] N. Shlezinger, S. Rini, and Y. C. Eldar, "The communication-aware clustered federated learning problem," in *Proc. IEEE ISIT*, 2020.
- [8] T. Li, A. K. Sahu, A. Talwalkar, and V. Smith, "Federated learning: Challenges, methods, and future directions," *IEEE Signal Process. Mag.*, vol. 37, no. 3, pp. 50–60, 2020.
- [9] speedtest.net, "Speedtest united states market report," 2019. [Online]. Available: <http://www.speedtest.net/reports/united-states/>
- [10] M. Chen, Z. Yang, W. Saad, C. Yin, H. V. Poor, and S. Cui, "A joint learning and communications framework for federated learning over wireless networks," *arXiv preprint arXiv:1909.07972*, 2019.
- [11] X. Li, K. Huang, W. Yang, S. Wang, and Z. Zhang, "On the convergence of fedavg on non-iid data," *arXiv preprint arXiv:1907.02189*.
- [12] D. Alistarh, D. Grubic, J. Li, R. Tomioka, and M. Vojnovic, "QSGD: Communication-efficient SGD via gradient quantization and encoding," in *Proc. NeurIPS*, 2017, pp. 1709–1720.
- [13] N. Shlezinger, M. Chen, Y. C. Eldar, H. V. Poor, and S. Cui, "UveQFed: Universal vector quantization for federated learning," *arXiv preprint arXiv:2006.03262*, 2020.
- [14] A. F. Aji and K. Heafield, "Sparse communication for distributed gradient descent," *arXiv preprint arXiv:1704.05021*, 2017.
- [15] D. Alistarh, T. Hoefler, M. Johansson, N. Konstantinov, S. Khirirat, and C. Renggli, "The convergence of sparsified gradient methods," in *Proc. NeurIPS*, 2018, pp. 5973–5983.
- [16] A. Goldsmith, *Wireless communications*. Cambridge Press, 2005.
- [17] M. M. Amiri and D. Gündüz, "Machine learning at the wireless edge: Distributed stochastic gradient descent over-the-air," *IEEE Trans. Signal Process.*, vol. 68, pp. 2155–2169, 2020.
- [18] —, "Federated learning over wireless fading channels," *IEEE Trans. Wireless Commun.*, vol. 19, no. 5, pp. 3546–3557, 2020.
- [19] T. Sery and K. Cohen, "On analog gradient descent learning over multiple access fading channels," *IEEE Trans. Signal Process.*, 2020.
- [20] K. Yang, T. Jiang, Y. Shi, and Z. Ding, "Federated learning via over-the-air computation," *IEEE Trans. Wireless Commun.*, vol. 19, no. 3, pp. 2022–2035, 2020.
- [21] H. Guo, A. Liu, and V. K. Lau, "Analog gradient aggregation for federated learning over wireless networks: Customized design and convergence analysis," *IEEE Internet Things J.*, 2020.
- [22] O. Abari, H. Rahul, and D. Katabi, "Over-the-air function computation in sensor networks," *arXiv preprint arXiv:1612.02307*, 2016.
- [23] G. Mergen and L. Tong, "Type based estimation over multiaccess channels," *IEEE Trans. Signal Process.*, vol. 54, no. 2, pp. 613–626, 2006.
- [24] G. Mergen, V. Naware, and L. Tong, "Asymptotic detection performance of type-based multiple access over multiaccess fading channels," *IEEE Trans. Signal Process.*, vol. 55, no. 3, pp. 1081–1092, Mar. 2007.
- [25] K. Liu and A. Sayeed, "Type-based decentralized detection in wireless sensor networks," *IEEE Trans. Signal Process.*, vol. 55, no. 5, pp. 1899–1910, May 2007.
- [26] S. Marano, V. Matta, T. Lang, and P. Willett, "A likelihood-based multiple access for estimation in sensor networks," *IEEE Trans. Signal Process.*, vol. 55, no. 11, pp. 5155–5166, Nov. 2007.
- [27] A. Anandkumar and L. Tong, "Type-based random access for distributed detection over multiaccess fading channels," *IEEE Trans. Signal Process.*, vol. 55, no. 10, pp. 5032–5043, 2007.
- [28] K. Cohen and A. Leshem, "Performance analysis of likelihood-based multiple access for detection over fading channels," *IEEE Trans. Inf. Theory*, vol. 59, no. 4, pp. 2471–2481, 2013.

- [29] I. Nevat, G. W. Peters, and I. B. Collings, "Distributed detection in sensor networks over fading channels with multiple antennas at the fusion centre," *IEEE Trans. Signal Process.*, vol. 62, no. 3, pp. 671–683, 2014.
- [30] P. Zhang, I. Nevat, G. W. Peters, and L. Clavier, "Event detection in sensor networks with non-linear amplifiers via mixture series expansion," *IEEE Sensors J.*, vol. 16, no. 18, pp. 6939–6946, 2016.
- [31] K. Cohen and A. Leshem, "Spectrum and energy efficient multiple access for detection in wireless sensor networks," *IEEE Trans. Signal Process.*, vol. 66, no. 22, pp. 5988–6001, 2018.
- [32] K. Cohen and D. Malachi, "A time-varying opportunistic multiple access for delay-sensitive inference in wireless sensor networks," *IEEE Access*, vol. 7, pp. 170 475–170 487, 2019.
- [33] M. Seif, R. Tandon, and M. Li, "Wireless federated learning with local differential privacy," *arXiv preprint arXiv:2002.05151*, 2020.
- [34] D. Liu and O. Simeone, "Privacy for free: Wireless federated learning via uncoded transmission with adaptive power control," *arXiv preprint arXiv:2006.05459*, 2020.
- [35] N. Cesa-Bianchi, S. Shalev-Shwartz, and O. Shamir, "Online learning of noisy data," *IEEE Trans. Inf. Theory*, vol. 57, no. 12, pp. 7907–7931, 2011.
- [36] S. U. Stich, "Local SGD converges fast and communicates little," *arXiv preprint arXiv:1805.09767*, 2018.
- [37] S. U. Stich, J.-B. Cordonnier, and M. Jaggi, "Sparsified SGD with memory," in *Proc. NeurIPS*, 2018, pp. 4447–4458.
- [38] T. Bertin-Mahieux, D. P. Ellis, B. Whitman, and P. Lamere, "The million song dataset," in *Proc. ISMIR*, 2011.
- [39] G. An, "The effects of adding noise during backpropagation training on a generalization performance," *Neural computation*, vol. 8, no. 3, pp. 643–674, 1996.
- [40] W.-T. Chang and R. Tandon, "Communication efficient federated learning over multiple access channels," *arXiv preprint arXiv:2001.08737*, 2020.
- [41] A. Neelakantan, L. Vilnis, Q. V. Le, I. Sutskever, L. Kaiser, K. Kurach, and J. Martens, "Adding gradient noise improves learning for very deep networks," *arXiv preprint arXiv:1511.06807*, 2015.
- [42] H. Chen, S. Lundberg, and S.-I. Lee, "Checkpoint ensembles: Ensemble methods from a single training process," *arXiv preprint arXiv:1710.03282*, 2017.
- [43] K. Cohen and A. Leshem, "A time-varying opportunistic approach to lifetime maximization of wireless sensor networks," *IEEE Trans. Signal Process.*, vol. 58, no. 10, pp. 5307–5319, 2010.
- [44] M. Lichman, "UCI machine learning repository," 2013. [Online]. Available: <http://archive.ics.uci.edu/ml>
- [45] MathWorks Deep Learning Toolbox Team, "Deep learning tutorial series," *MATLAB Central File Exchange*, 2020. [Online]. Available: <https://www.mathworks.com/matlabcentral/fileexchange/62990-deep-learning-tutorial-series>